

Mobility anisotropy of two-dimensional semiconductors

Haifeng Lang,¹ Shuqing Zhang,² and Zhirong Liu^{1,2,3,*}¹College of Chemistry and Molecular Engineering, Peking University, Beijing 100871, China²Center for Nanochemistry, Academy for Advanced Interdisciplinary Studies, Peking University, Beijing 100871, China³State Key Laboratory for Structural Chemistry of Unstable and Stable Species, Beijing National Laboratory for Molecular Sciences, Peking University, Beijing 100871, China

(Received 11 July 2016; revised manuscript received 26 November 2016; published 23 December 2016)

The carrier mobility of anisotropic two-dimensional semiconductors under longitudinal acoustic phonon scattering was theoretically studied using deformation potential theory. Based on the Boltzmann equation with the relaxation time approximation, an analytic formula of intrinsic anisotropic mobility was derived, showing that the influence of effective mass on mobility anisotropy is larger than those of deformation potential constant or elastic modulus. Parameters were collected for various anisotropic two-dimensional materials (black phosphorus, Hittorf's phosphorus, BC₂N, MXene, TiS₃, and GeCH₃) to calculate their mobility anisotropy. It was revealed that the anisotropic ratio is overestimated by the previously described method.

DOI: 10.1103/PhysRevB.94.235306

I. INTRODUCTION

The successful isolation of graphene in 2004 [1] led us into the brand new world of two-dimensional (2D) materials [2,3]. As the lecture title given by Richard P. Feynman in 1959 states [4], "There's plenty of room at the bottom." Since graphene was born, unforeseen physical and chemical properties of this atomically thin material have quickly attracted attention [5,6]. For example, unique ballistic transport and extraordinarily high carrier mobility have greatly expanded graphene's potential applications [7,8]. However, graphene has its own drawback: It is semimetal with a zero band gap, which severely limits its potential in electronic applications where a moderate gap is required [9]. Therefore, many studies have explored other 2D materials beyond graphene [10,11]. Representative semiconducting 2D systems include graphynes [12–14], transition metal dichalcogenides (TMDs) (such as MoS₂, MoSe₂, and WSe₂) [15,16], black phosphorus (BP) [17,18], and transition metal carbides and nitrides (MXenes) [19,20]. Taking BP as an example, inside a single layer, each P atom is covalently bonded with three adjacent P atoms to form a strongly puckered honeycomb structure with troughs running in a zigzag direction [17,21,22]. Due to the puckering, bonds in BP are divided into two inequivalent types, a sharp contrast to the completely planar honeycomb structure of graphene where all bonds are equivalent. As a result, BP processes a nonzero band gap between 0.3 eV and 2 eV depending on the thickness, and the charge-carrier mobility is retained up to about 1000 cm² V⁻¹ s⁻¹ [17,21]. These unusual properties provide new opportunities for future electronic and photonic devices.

Some 2D materials are isotropic [15,23–25] while others are anisotropic [17–20]. In anisotropic 2D semiconductors, the electrons and phonons behave differently in different planar directions, leading to angle-dependent mechanical, optical, and electrical responses. These unique properties may permit the design of novel sensors with anisotropic crystalline orientation, optical absorption and scattering, carrier mobility, and electronic conductance [22,25–27]. In the present study,

we focus on the theoretical study of the anisotropic carrier mobility.

Despite the importance of carrier mobility, the theory of intrinsic mobility for anisotropic 2D semiconductors is not well developed. The widely used mobility formula in literature is based on the deformation potential theory proposed by Bardeen and Shockley in 1950, where the acoustic phonon limited mobility of an isotropic three-dimensional (3D) non-polar semiconductor was given as [28]:

$$\mu = \frac{2\sqrt{2\pi}e\hbar^4 C^{(3D)}}{3m^{\frac{5}{2}}(k_B T)^{\frac{3}{2}} E_1^2}, \quad (1)$$

where m is the effective mass of charge carriers (electrons and holes), $C^{(3D)} = C_{11}^{(3D)} \equiv C_{22}^{(3D)} \equiv C_{33}^{(3D)}$ is the isotropic elastic constant, and E_1 is the deformation potential constant defined as the energy shift of the band edge position with respect to the uniaxial strain. Then Kawaji extended the theory to the 2D electron gas (2DEG) system in 1969 [29]. Later, the effect of anisotropic mass was added into the theory [30,31], and the resulting 2D mobility can be given as:

$$\begin{aligned} \mu_x &= \frac{e\hbar^3 C^{(2D)}}{k_B T (m_x)^{\frac{3}{2}} (m_y)^{\frac{1}{2}} E_1^2} \\ \mu_y &= \frac{e\hbar^3 C^{(2D)}}{k_B T (m_x)^{\frac{1}{2}} (m_y)^{\frac{3}{2}} E_1^2}. \end{aligned} \quad (2)$$

In recent studies of anisotropic 2D semiconductors, however, Eq. (2) has been arbitrarily generalized to include the effects of anisotropic C and E_1 [17,19,32,33]:

$$\begin{aligned} \mu_x &= \frac{e\hbar^3 C_{11}^{(2D)}}{k_B T (m_x)^{\frac{3}{2}} (m_y)^{\frac{1}{2}} E_{1x}^2} \\ \mu_y &= \frac{e\hbar^3 C_{22}^{(2D)}}{k_B T (m_x)^{\frac{1}{2}} (m_y)^{\frac{3}{2}} E_{1y}^2}. \end{aligned} \quad (3)$$

Equation (3) implies that the mobility in a specified direction is determined only by C and E_1 in the same direction but is independent of those in the perpendicular direction. Actually,

*liuzhirong@pku.edu.cn

this is logically incorrect, because moving carriers would be inevitably scattered by phonons from all directions.

The rest of this paper is organized as follows. In Sec. II, a historic perspective on the mobility of 2DEG is provided to demonstrate its relation to that of 2D materials. In Sec. III, the contributions of anisotropic m , C , and E_1 on mobility μ are theoretically studied separately. In Sec. IV, the obtained formula is applied to numerically analyze the mobility anisotropy of some 2D materials, showing that the anisotropy in most systems is weaker than previously thought. Finally, we summarize our results and conclusions in Sec. V.

II. HISTORICAL PERSPECTIVE

To understand the state of the art in mobility calculations in anisotropic 2D semiconductors using deformation potential theory, it is necessary to understand the historical development. In this section, we make a brief review of the literature and identify some improper ways in mobility calculations.

The deformation potential theory was first proposed by Bardeen and Shockley in 1950 for three-dimensional (3D) nonpolar semiconductors [28]. With the development of metal-oxide-semiconductor field-effect transistors (MOSFETs) in the following years, scientists found that the electrons move freely in two dimensions at the semiconductor-oxide interface of MOSFETs, but are tightly confined in the third dimension, which can be described as a 2D sheet embedded in a 3D world. All constructs with similar characteristics became known as 2DEG [29,34]. In 1969, Kawaji extended the deformation potential theory to the phonon-limited carrier mobility of 2DEG in a semiconductor inversion layer by an inverted triangular well potential model, and a simple formula was reported to calculate the lattice-scattering mobility of 2DEG [29]:

$$\mu = \frac{e\hbar^3 \rho^{(3D)} v_l^2}{m^2 k_B T E_1^2} \cdot W_{\text{eff}}, \quad (4)$$

where $\rho^{(3D)}$ is the 3D mass density of the crystal, v_l is the velocity of the longitudinal wave, and ρv_l^2 can be replaced by 3D elastic constant $C_{11}^{(3D)}$. W_{eff} is the effective thickness of the inversion layer with a complex expression determined by the dielectric constant of the material as well as the impurity and free electron densities [28,29]. Then in 1981, Price applied the theory in a semiconductor heterolayer to calculate lattice-scattering mobility [35]. He described the layer for active carriers in 2DEG as square wells, obtaining a simple expression for W_{eff} :

$$W_{\text{eff}} = \frac{2}{3} L, \quad (5)$$

where L is the width of the square well [35]. In anisotropic systems, effective mass m and deformation potential constant E_1 are second-order tensors, whereas elastic modulus C is a fourth-order tensor, components of these tensors are not independent [36]. The mobility anisotropy of 2DEG on oxidized silicon surfaces could be attributed to the difference in the effective mass. This was explored by Satô *et al.* in 1971 based on an ellipsoidal constant-energy surface [34]. With the anisotropic mass, the mobility of 2DEG in the inversion layer

was modified into [30,31]

$$\mu_x = \frac{e\hbar^3 \rho^{(3D)} v_l^2}{m_x m_d k_B T E_1^2} \cdot W_{\text{eff}}, \quad (6)$$

where $m_d = \sqrt{m_x m_y}$.

2DEG in an inversion layer is not a real 2D system, in the sense that it is always embedded in 3D material. Thus, 3D parameter $\rho^{(3D)}$ appears in Eqs. (4) and (6). Graphene and other 2D crystals studied in recent years, however, are real 2D systems since they could exist independently. As an important property, their mobility attracted a lot of interest [16,17,23,37,38]. Almost all of the mobility calculations were based on the generation of Eqs. (4) and (6) of 2DEG. To generate the formula to real 2D systems, some studies assumed $\rho^{(3D)} W_{\text{eff}} = \rho^{(2D)}$ to give [24,31,37,39]

$$\mu_x = \frac{e\hbar^3 \rho^{(2D)} v_l^2}{m_x m_d k_B T E_1^2} = \frac{e\hbar^3 C_{11}^{(2D)}}{m_x m_d k_B T E_1^2}, \quad (7)$$

while others assumed $\rho^{(3D)} L = \rho^{(2D)}$ to give [20,40–42]

$$\mu_x = \frac{2e\hbar^3 \rho^{(2D)} v_l^2}{3m_x m_d k_B T E_1^2} = \frac{2e\hbar^3 C_{11}^{(2D)}}{3m_x m_d k_B T E_1^2}. \quad (8)$$

These generated formulas are somewhat arbitrary without necessary theoretical deduction. For example, the factor 2/3 comes from 2DEG being confined in a square well, but the behaviors of electrons in real 2D systems are unrelated to square wells. Therefore, Eq. (7) is valid when both deformation potential and elastic modulus are isotropic, whereas Eq. (8) is always invalid. Another false assumption in the literature lay is the anisotropic effects. Equation (7) was originally used to investigate the mobility of an isotropic system such as 2D hexagonal BN [38] but was later adopted to study anisotropic systems such as BP [17,22]. As we will show in the next sections, Eqs. (3), (7), and (8) are not applicable under anisotropic deformation potential and elastic modulus.

III. THEORETICAL ANALYSES ON THE ANISOTROPIC MOBILITY

A. General consideration

Carrier mobility of a sample is determined by various scattering processes whose effects are influenced by temperature and carrier density. The scattering caused by defects and impurities is insensitive to temperature and carrier density and can be eliminated or reduced significantly by improving sample preparation. The scattering caused by electron-electron interaction increases with increasing carrier density. For high-quality materials when the carrier density is not too high, the primary source of scattering comes from phonons [28]. At low temperatures, because the high-energy optical phonons cannot be excited, the acoustic phonons dominate the scattering process. For example, the resistivity of graphene for $T < 200$ K is mainly determined by acoustic phonons [43–45]. This scattering by acoustic phonons cannot be eliminated at finite temperatures and thus determines the intrinsic mobility of the material. In the present study, we focus on the effects of acoustic phonon scattering, which is expected to be important at low temperatures between approximately 10 K and 200 K.

Theoretically, the intrinsic mobility caused by acoustic phonons can be described by deformation potential theory [28], where the atomic displacement associated with a long-wavelength acoustic phonon leads to a deformation of the crystal, and in turn, to a shift of the band edge and scattering between different eigenstates. In the spirit of the deformation potential theory, the shift of the band edge (ΔE_{edge}) is proportional to the longitudinal strain $\varepsilon(\mathbf{q})$ caused by longitudinal acoustic vibrational modes (phonons) with a wave vector \mathbf{q} :

$$\Delta E_{\text{edge}} = E_1(\mathbf{q})\varepsilon(\mathbf{q}), \quad (9)$$

where the deformation potential constant E_1 depends on the direction of longitudinal strain and phonons for anisotropic materials. The contribution of transverse acoustic phonons is ignored as in the usual deformation potential theory. Under Fermi's golden rule and the second quantization of the phonons, the scattering probability of an electron from eigenstate \mathbf{k} to \mathbf{k}' caused by longitudinal acoustic phonons depends on the scattering matrix element, which was obtained by Bardeen and Shockley for 3D cases [28] and later by Price for 2D cases [35]:

$$W_{\mathbf{k},\mathbf{k}'} = \frac{2\pi k_B T E_1(\mathbf{q})^2}{A \hbar C(\mathbf{q})} \delta(\varepsilon_{\mathbf{k}} - \varepsilon_{\mathbf{k}'}), \quad (10)$$

where A is the area of 2D sample and $C(\mathbf{q})$ is the elastic modulus caused by $\varepsilon(\mathbf{q})$. The superscript “(2D)” in the formula is omitted hereafter. The momentum conservation law requires that $\mathbf{q} = \mathbf{k}' - \mathbf{k}$. Both the emission and the absorption of the phonons were considered in obtaining Eq. (10). The equipartition principle was also adopted here, which limits Eq. (10) to be applicative only above the characteristic degenerate (Bloch-Grüneisen) temperature (usually a few tens of K). The relaxation time for an electron in \mathbf{k} , denoted as $\tau(\mathbf{k})$, is thus given by

$$\frac{1}{\tau(\mathbf{k})} = \frac{A}{4\pi^2} \int W_{\mathbf{k},\mathbf{k}'} \left(1 - \frac{\mathbf{v}_{\mathbf{k}} \cdot \mathbf{v}_{\mathbf{k}'}}{|\mathbf{v}_{\mathbf{k}}|^2} \right) d^2\mathbf{k}', \quad (11)$$

where $\mathbf{v}_{\mathbf{k}}$ is the group velocity. The Boltzmann equation is the basis for the classical and semiclassical theories of transport processes. It has been widely used in studying thermal, mass, and electrical conductivities under weak driving forces. Based on the Boltzmann equation with the relaxation time approximation, the 2D conductivity tensor is solved to be [24,46,47]

$$\tilde{\sigma} = 2e^2 \int \tau(\mathbf{k}) \frac{\partial n_F(\varepsilon_{\mathbf{k}})}{\partial \varepsilon_{\mathbf{k}}} \mathbf{v}_{\mathbf{k}} \mathbf{v}_{\mathbf{k}} \frac{d^2\mathbf{k}}{(2\pi)^2}, \quad (12)$$

where $\varepsilon_{\mathbf{k}}$ is the eigenenergy of state \mathbf{k} , and $n_F(\varepsilon_{\mathbf{k}})$ is the equilibrium Fermi-Dirac distribution. The mobility along the x direction is thus

$$\mu_x = \frac{\sigma_{xx}}{ne}, \quad (13)$$

where $n = 2 \int n_F(\varepsilon_{\mathbf{k}}) \frac{d^2\mathbf{k}}{(2\pi)^2}$ is the carrier density. Equations (9)–(13) provide the general framework to calculate the intrinsic mobility of 2D materials under longitudinal acoustic phonons. The mobility anisotropy may arise from anisotropic $\varepsilon_{\mathbf{k}}$ (which is related to the anisotropic effective mass), $E_1(\mathbf{q})$ or $C(\mathbf{q})$, which will be analyzed in detail as follows.

B. Anisotropic mass

When only the effective mass is anisotropic, the energy dispersion is described as

$$\varepsilon_{\mathbf{k}} = \frac{\hbar^2 k_x^2}{2m_x} + \frac{\hbar^2 k_y^2}{2m_y}, \quad (14)$$

where the x and y directions are chosen to be along the primary axes of the energy dispersion. Making use of the coordinate transformation

$$\begin{aligned} \tilde{k}_x &= \frac{k_x}{\sqrt{m_x}} \\ \tilde{k}_y &= \frac{k_y}{\sqrt{m_y}}, \end{aligned} \quad (15)$$

it is straightforward to derive from Eqs. (9)–(13) to get the relaxation time

$$\tau(\mathbf{k}) = \frac{\hbar^3 C_{11}}{k_B T E_1^2 \sqrt{m_x m_y}}, \quad (16)$$

and the mobility

$$\mu_x = \frac{e \hbar^3 C_{11}}{k_B T E_1^2 (m_x)^{\frac{3}{2}} (m_y)^{\frac{1}{2}}}, \quad (17)$$

where $E_1 \equiv E_1(\mathbf{q})$ and $C_{11} \equiv C(\mathbf{q})$ are isotropic. $\tau(\mathbf{k})$ is independent on \mathbf{k} even if the effective mass is anisotropic in this case. Equation (17) is identical to Eq. (2), and it is also the same as Eq. (3) if both $C^{(\text{tr})}$ and $E_1^{(\text{tr})}$ are isotropic, that is, Eq. (3) is valid when only the effective mass is anisotropic.

C. Elliptic deformation potential

We now consider the case that only the deformation potential is anisotropic while both effective mass and elastic modulus remain isotropic. As a second-order tensor, any strain can be decomposed into three components in 2D systems: two uniaxial strains (ε_x and ε_y along the x and y directions, respectively) and a shear strain (γ). Under a first-order approximation, the shift of the band edge caused by any strain can be decomposed into

$$\Delta E_{\text{edge}} = E_{1x}\varepsilon_x + E_{1y}\varepsilon_y + E_{1\gamma}\gamma, \quad (18)$$

where E_{1x} , E_{1y} , and $E_{1\gamma}$ are three components of the deformation potential constants. The effective deformation potential constant $E_1(\mathbf{q})$ under a longitudinal strain along any specified direction as defined in Eq. (9) can be deduced with the Herring-Vogt transformation [48] as explained here. Denoting the magnitude and the directional angle of the longitudinal strain as ε and $\theta_{\mathbf{q}}$, with the tensor transformation under rotation, the longitudinal strain is expressed in a tensor form of

$$\begin{aligned} \tilde{\varepsilon}(\mathbf{q}) &\equiv \begin{bmatrix} \varepsilon_x & \gamma \\ \gamma & \varepsilon_y \end{bmatrix} = \mathbf{R}^T \begin{bmatrix} \varepsilon & 0 \\ 0 & 0 \end{bmatrix} \mathbf{R} \\ &= \begin{bmatrix} \varepsilon \cos^2 \theta_{\mathbf{q}} & -\varepsilon \sin \theta_{\mathbf{q}} \cos \theta_{\mathbf{q}} \\ -\varepsilon \sin \theta_{\mathbf{q}} \cos \theta_{\mathbf{q}} & \varepsilon \sin^2 \theta_{\mathbf{q}} \end{bmatrix}, \end{aligned} \quad (19)$$

where \mathbf{R} is the 2D rotation matrix:

$$\mathbf{R} = \begin{bmatrix} \cos \theta_{\mathbf{q}} & \sin \theta_{\mathbf{q}} \\ -\sin \theta_{\mathbf{q}} & \cos \theta_{\mathbf{q}} \end{bmatrix}. \quad (20)$$

Substituting Eq. (19) into Eq. (18), yields

$$\begin{aligned} \Delta E_{\text{edge}}(\vec{\varepsilon}(\mathbf{q})) &\equiv \Delta E_{\text{edge}}(\varepsilon, \theta_{\mathbf{q}}) \\ &= (E_{1x} \cos^2 \theta_{\mathbf{q}} + E_{1y} \sin^2 \theta_{\mathbf{q}} - 2E_{1y} \sin \theta_{\mathbf{q}} \cos \theta_{\mathbf{q}}) \varepsilon. \end{aligned} \quad (21)$$

If the system has mirror reflection symmetry, by setting the mirror plane (line) as the x direction, it requires

$$\Delta E_{\text{edge}}(\varepsilon, -\theta_{\mathbf{q}}) = \Delta E_{\text{edge}}(\varepsilon, \theta_{\mathbf{q}}), \quad (22)$$

which results in $E_{1y} = 0$. In this case, the contribution of the shear component to the deformation potential disappears, then $E_1(\mathbf{q})$ becomes

$$E_1(\mathbf{q}) = E_{1x} \cos^2 \theta_{\mathbf{q}} + E_{1y} \sin^2 \theta_{\mathbf{q}}. \quad (23)$$

Combined with Eqs. (10) and (23), the integration in Eq. (11) gives

$$\frac{1}{\tau(\mathbf{k})} = \frac{mk_B T}{\hbar^3 C_{11}} \left[\bar{E}_1^2 + \frac{(\Delta E_1)^2}{2} - \bar{E}_1 \Delta E_1 \cos(2\theta_{\mathbf{k}}) \right], \quad (24)$$

where $\theta_{\mathbf{k}}$ is the polar angle of \mathbf{k} , while \bar{E}_1 and ΔE_1 are notations defined as

$$\begin{aligned} \bar{E}_1 &= \frac{E_{1y} + E_{1x}}{2} \\ \Delta E_1 &= \frac{E_{1y} - E_{1x}}{2}. \end{aligned} \quad (25)$$

$\tau(\mathbf{k})$ is anisotropic here, being distinct from the result of Eq. (16) under anisotropic effective mass. The mobility is obtained as

$$\begin{aligned} \mu_x &= \frac{e \int \frac{\hbar^3 C_{11}}{mk_B T} \cdot \frac{k^2 \cos^2 \theta_{\mathbf{k}}}{\bar{E}_1^2 + \frac{(\Delta E_1)^2}{2} - \bar{E}_1 \Delta E_1 \cos(2\theta_{\mathbf{k}})} \cdot \frac{\hbar^2}{m^2} \cdot \frac{\partial n_F(\varepsilon_{\mathbf{k}})}{\partial \varepsilon_{\mathbf{k}}} d^2 \mathbf{k}}{\int \frac{\partial n_F(\varepsilon_{\mathbf{k}})}{\partial \varepsilon_{\mathbf{k}}} d^2 \mathbf{k}} \\ &= \frac{e \hbar^3 C_{11}}{m^2 k_B T} \left(\frac{A + B - \sqrt{A^2 - B^2}}{B \sqrt{A^2 - B^2}} \right), \end{aligned} \quad (26)$$

with the notations

$$\begin{aligned} A &= \bar{E}_1^2 + \frac{(\Delta E_1)^2}{2} \\ B &= \bar{E}_1 \Delta E_1. \end{aligned} \quad (27)$$

Equation (26) is a bit complicated. To see the anisotropic effect more clearly, we rewrite it as

$$\mu_x = \frac{e \hbar^3 C_{11}}{m^2 k_B T \bar{E}_1^2} \times \frac{1}{f\left(\frac{\Delta E_1}{\bar{E}_1}\right)}, \quad (28)$$

where $f\left(\frac{\Delta E_1}{\bar{E}_1}\right)$ is a corrected factor due to the anisotropic effect:

$$f\left(\frac{\Delta E_1}{\bar{E}_1}\right) = \frac{1}{\bar{E}_1^2} \times \frac{B \sqrt{A^2 - B^2}}{A + B - \sqrt{A^2 - B^2}}. \quad (29)$$

The curve of $f\left(\frac{\Delta E_1}{\bar{E}_1}\right)$ is given in Fig. 1. Setting $\Delta E_1 = 0$ gives $f = 1$, consistent with the isotropic result. Within the

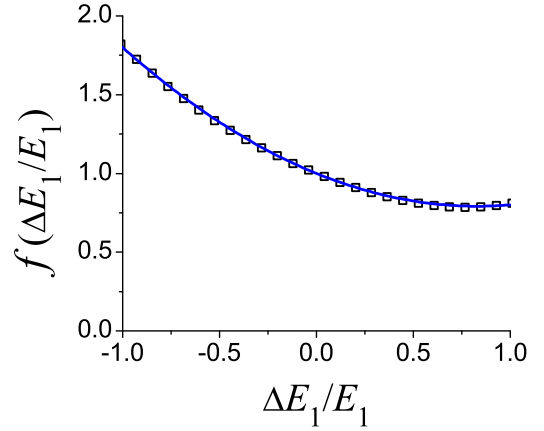


FIG. 1. The corrected factor $f\left(\frac{\Delta E_1}{\bar{E}_1}\right)$ due to the anisotropic deformation potential. Scattering points were calculated with Eq. (29), while the solid line is a quadratic approximation as given in Eq. (30).

examined range, $f\left(\frac{\Delta E_1}{\bar{E}_1}\right)$ can be well reproduced by a quadratic function:

$$f\left(\frac{\Delta E_1}{\bar{E}_1}\right) = 1 - 0.5 \frac{\Delta E_1}{\bar{E}_1} + 0.3 \left(\frac{\Delta E_1}{\bar{E}_1} \right)^2, \quad (30)$$

as demonstrated as the solid line in Fig. 1. With the quadratic approximation, the mobility under anisotropic deformation potential is simplified as

$$\mu_x = \frac{e \hbar^3 C_{11}}{m^2 k_B T \left(\frac{9E_{1x}^2 + 7E_{1x}E_{1y} + 4E_{1y}^2}{20} \right)}. \quad (31)$$

D. Elliptic elastic constant

The anisotropic effect of elastic modulus $C(\mathbf{q})$, theoretically speaking, can be expressed in terms of the complete 2D elastic constants ($C_{11}, C_{22}, C_{66}, C_{26}, C_{16}, C_{12}$) using the elastic theory. However, usually only the values of C_{11} and C_{22} along the primary axes are used in the literature for mobility calculation. As an approximation, we express $C(\mathbf{q})$ as a function of only C_{11} and C_{22} . Obviously, $C(\mathbf{q})$ should have the following properties: (1) $C(\mathbf{q}) = C_{11}$ for a strain applying along the x axis; (2) $C(\mathbf{q}) = C_{22}$ for a strain applying along the y axis; (3) $C(\mathbf{q})$ is isotropic when $C_{11} = C_{22}$. A simple approximated expression satisfying the requirements is adopted here as:

$$C(\mathbf{q}) = C_{11} \cos^2 \theta_{\mathbf{q}} + C_{22} \sin^2 \theta_{\mathbf{q}}. \quad (32)$$

The effective mass and deformation potential are kept isotropic. The relaxation time is obtained as:

$$\frac{1}{\tau(\mathbf{k})} = \frac{mk_B T E_1^2}{\hbar^3} \left[\frac{1 + \frac{\bar{C}}{\Delta C} \cos(2\theta_{\mathbf{k}})}{\sqrt{\bar{C}^2 - (\Delta C)^2}} - \frac{\cos(2\theta_{\mathbf{k}})}{\Delta C} \right], \quad (33)$$

where

$$\begin{aligned} \bar{C} &= \frac{C_{11} + C_{22}}{2} \\ \Delta C &= \frac{C_{22} - C_{11}}{2}. \end{aligned} \quad (34)$$

The mobility is given as

$$\mu_x = \frac{\int \frac{e\hbar^5}{m^3 k_B T E_1^2} \cdot \frac{k^2 \cos^2 \theta_k}{\sqrt{\bar{C}^2 - (\Delta C)^2} - \frac{\bar{C}}{\Delta C} \left(\frac{1}{\bar{C}} - \frac{1}{\sqrt{\bar{C}^2 - (\Delta C)^2}} \right) \cos(2\theta_k)} \cdot \frac{\partial n_F(\epsilon_k)}{\partial \epsilon_k} d^2 \mathbf{k}}{\int \frac{\partial n_F(\epsilon_k)}{\partial \epsilon_k} d^2 \mathbf{k}}$$

$$= \frac{e\hbar^3}{m^2 k_B T E_1^2} \left(\frac{I + J - \sqrt{I^2 - J^2}}{J \sqrt{I^2 - J^2}} \right), \quad (35)$$

where

$$I = \frac{1}{\sqrt{\bar{C}^2 - (\Delta C)^2}}$$

$$J = \frac{\bar{C}}{\Delta C} \left(\frac{1}{\bar{C}} - \frac{1}{\sqrt{\bar{C}^2 - (\Delta C)^2}} \right). \quad (36)$$

Equation (35) can be expanded to the linear order of ΔC to give a simplified result:

$$\mu_x = \frac{e\hbar^3}{m^2 k_B T E_1^2} \left(\frac{5C_{11} + 3C_{22}}{8} \right), \quad (37)$$

which shows that the mobility along the x direction depends on the elastic constants along both x and y directions.

IV. RESULTS AND DISCUSSION

A. Combined anisotropic effects on mobility

In the section above, the anisotropic effects of the effective mass, the deformation potential, and the elastic modulus on the mobility of 2D semiconductors were analyzed separately to give analytical results. When all these anisotropic factors appear together in a system, it is too complex to achieve an analytical solution. Therefore, we propose expressing the mobility approximately by combining different anisotropic factors directly:

$$\mu_x = \frac{e\hbar^3}{k_B T (m_x)^{\frac{3}{2}} (m_y)^{\frac{1}{2}}} \left(\frac{A + B - \sqrt{A^2 - B^2}}{B \sqrt{A^2 - B^2}} \right) \times \left(\frac{I + J - \sqrt{I^2 - J^2}}{J \sqrt{I^2 - J^2}} \right), \quad (38)$$

where A and B are functions of deformation potential whose definition was given in Eq. (27), while I and J are functions of elastic modulus, whose definition was given in Eq. (36). With the low order approximation, a concise form is achieved as:

$$\mu_x = \frac{e\hbar^3 \left(\frac{5C_{11} + 3C_{22}}{8} \right)}{k_B T (m_x)^{\frac{3}{2}} (m_y)^{\frac{1}{2}} \left(\frac{9E_{1x}^2 + 7E_{1x}E_{1y} + 4E_{1y}^2}{20} \right)}. \quad (39)$$

Anisotropic effective mass is the main contributor to the mobility anisotropy. To measure the mobility anisotropy, we define an anisotropic ratio R_{ani} as:

$$R_{\text{ani}} = \frac{\max(\mu_x, \mu_y)}{\min(\mu_x, \mu_y)}, \quad (40)$$

which is equal to 1.0 for isotropic systems and is larger than 1.0 for anisotropic systems. The variation of R_{ani} with various parameters is demonstrated in Fig. 2. Anisotropic

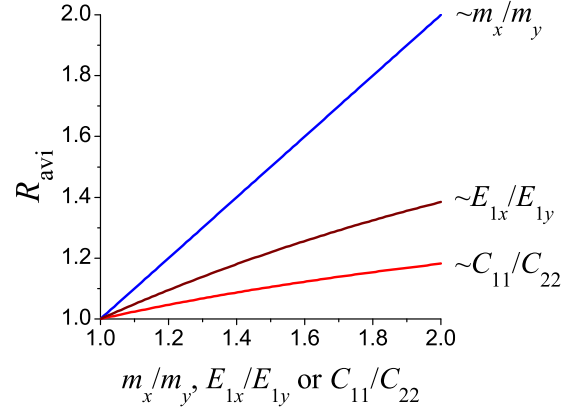


FIG. 2. Anisotropic ratio of mobility (R_{ani}) as functions of $\frac{m_x}{m_y}$, $\frac{E_{1x}}{E_{1y}}$, and $\frac{C_{11}}{C_{22}}$. Results are calculated with Eq. (39). Except the parameter being varied in each line, $\frac{m_x}{m_y} = 1$, $\frac{E_{1x}}{E_{1y}} = 1$, $\frac{C_{11}}{C_{22}} = 1$.

mass acting along with $\frac{m_x}{m_y} = 2$ yields $R_{\text{ani}} = 2.0$. In contrast, $R_{\text{ani}} = 1.18$ for $\frac{C_{11}}{C_{22}} = 2$ and $R_{\text{ani}} = 1.38$ for $\frac{E_{1x}}{E_{1y}} = 2$. Therefore, the anisotropy contribution from elastic constant and deformation potential is much weaker than that from the energy dispersion (effective mass). Consistently, for materials with Dirac cone and zero band gap, the anisotropic contribution is also dominated by the energy dispersion (Fermi velocity) while the contribution from deformation potential is nearly zero [3,46,49].

B. Numerical results

To numerically evaluate the mobility anisotropy of 2D semiconductors, and to examine how the new formulas [Eqs. (38) and (39)] produce results differently from the old one [Eq. (3)], data for various anisotropic materials were collected from the literature, including BP [17], single-layer Hittorf's phosphorus (HP) [33], BC_2N [32], TiS_3 [40,41], GeCH_3 [42], Ti_2CO_2 [19,20], Hf_2CO_2 [19], Zr_2CO_2 [19], Sc_2CF_2 , and $\text{Sc}_2\text{C}(\text{OH})_2$ [50]. Analysis results for some representative systems are listed in Table I. For these systems, Eq. (38) and Eq. (39) give very close results, suggesting the simplified Eq. (39) is a good approximation of the full form of Eq. (38). However, the difference between new and old methods is distinct, as discussed below.

Undoped BP is p -type semiconductor. Related experiments on thin-layer BP have suggested that hole mobility is larger than electron mobility, and that mobility along the x (armchair) direction is greater than that along the y direction [18,51–53]. However, calculations for single-layer BP using the old formula have given contrasting results of $\mu_x(\text{h}) < \mu_x(\text{e})$ and $\mu_x(\text{h}) < \mu_y(\text{h})$, as shown in Table I. Conversely, under the same parameters, the new formula produces results more consistent with experiments. There is a discrepancy between the old and new formulas because the old formula overestimates the contribution of the deformation potential to the mobility anisotropy. This leads to a prediction that the anisotropy ratio is proportional to $\left(\frac{E_{1y}}{E_{1x}}\right)^2$ [see Eq. (3)]. Because single-layer BP has E_{1x} ($= 2.5$ eV) much larger than E_{1y} ($= 0.15$ eV) for

TABLE I. Predicted mobility anisotropy of some representative 2D semiconductors.

System		m_x	m_y	E_{1x}	E_{1y}	C_{11}	C_{22}	old			new			simplified		
								μ_x	μ_y	R_{ani}	μ_x	μ_y	R_{ani}	μ_x	μ_y	R_{ani}
BP [17]	e	0.17	1.12	2.72	7.11	28.9	102	1.12	0.08	14.0	0.69	0.09	7.40	0.80	0.40	7.64
	h	0.15	6.35	2.5	0.15	28.9	102	0.67	16.0	23.9	2.37	0.16	14.6	2.77	0.18	15.1
2-BP [17]	e	0.18	1.13	5.02	7.35	57.5	195	0.60	0.15	4.00	0.81	0.14	5.58	0.70	0.13	5.76
	h	0.15	1.81	2.45	1.63	57.5	195	2.70	1.80	1.50	6.40	0.85	7.28	5.53	0.76	7.52
3-BP [17]	e	0.16	1.15	5.85	7.63	85.9	287	0.78	0.21	3.71	1.17	0.19	6.06	1.01	0.17	6.25
	h	0.15	1.12	2.49	2.24	85.9	287	4.80	2.70	1.78	9.72	1.80	5.24	8.41	1.61	5.40
4-BP [17]	e	0.16	1.16	5.92	7.58	115	379	1.02	0.28	3.64	1.54	0.25	6.08	1.33	0.22	6.26
	h	0.14	0.97	3.16	2.79	115	379	4.80	2.90	1.66	9.66	1.94	4.83	8.38	1.74	4.97
5-BP [17]	e	0.15	1.18	5.79	7.53	146	480	1.47	0.38	3.87	2.19	0.32	6.66	1.91	0.29	6.86
	h	0.14	0.89	3.40	2.97	146	480	5.90	3.80	1.55	11.1	2.45	4.42	9.68	2.19	4.55
HP [33]	e	0.69	3.58	1.40	0.66	49.7	49.9	0.50	0.43	1.16	0.76	0.21	3.65	0.76	0.21	3.65
	h	1.24	2.45	1.26	0.18	49.7	49.9	0.31	7.68	24.8	0.61	0.60	1.01	0.62	0.61	1.01
BC ₂ N [32]	e	0.15	0.41	1.87	4.25	307	400	52.5	3.70	14.2	22.3	5.59	3.98	22.1	5.56	3.97
	h	0.16	2.22	2.13	4.33	307	400	14.8	0.27	54.9	7.66	0.40	19.3	7.62	0.39	19.3
2-BC ₂ N [32]	e	0.16	0.40	1.86	4.13	771	769	118	9.61	12.3	52.9	14.6	3.62	52.2	14.7	3.61
	h	0.18	0.58	2.15	4.21	771	769	60.5	4.95	12.2	32.0	7.24	4.43	32.2	7.27	4.43
3-BC ₂ N [32]	e	0.17	0.41	0.79	2.79	1023	901	809	23.4	34.5	177	42.3	4.22	179	42.5	4.20
	h	0.20	0.66	3.41	2.82	1023	901	27.0	10.3	2.62	28.1	9.06	3.10	28.0	9.05	3.10
4-BC ₂ N [32]	e	0.17	0.42	0.95	3.30	1254	1285	651	22.4	29.1	161	39.1	4.14	163	39.3	4.12
	h	0.21	0.87	2.80	3.47	1254	1285	37.7	6.15	6.13	32.1	7.01	4.58	32.1	7.02	4.58
5-BC ₂ N [32]	e	0.18	0.43	2.0	0.88	1856	1571	200	364	1.81	289	169	1.71	290	170	1.71
	h	0.23	1.0	3.44	2.63	1856	1571	31.3	10.2	3.06	34.2	8.61	3.97	34.1	8.59	3.97
Ti ₂ CO ₂ [19]	e	0.38	3.03	9.17	4.71	253	256	0.15	0.07	2.08	0.23	0.04	5.83	0.23	0.04	5.84
	h	0.09	0.13	3.25	5.28	253	256	50.1	12.8	3.91	34.1	17.9	1.90	34.1	18.0	1.90
Ti ₂ CO ₂ [20]	e	0.44	4.53	5.71	0.85	267	265	0.61	0.25	2.41	0.56	0.11	5.31	0.55	0.10	5.34
	h	0.14	0.16	1.66	2.60	267	265	74.1	22.5	3.29	66.1	46.4	1.43	65.9	46.3	1.42
TiS ₃ [40]	e	1.47	0.41	0.73	0.94	81.3	145	1.01	13.9	13.7	2.89	10.6	3.66	2.99	10.9	3.64
	h	0.32	0.98	3.05	-3.8	81.3	145	1.12	0.15	8.07	2.30	0.71	3.26	4.16	1.12	3.73
GeCH ₃ [42]	e	0.03	0.19	12.7	12.5	51.7	49.6	6.71	0.12	53.7	3.71	0.51	7.31	3.72	0.51	7.31
	h	0.04	0.31	6.24	6.28	51.7	49.6	14.0	0.19	75.3	7.07	0.83	8.56	7.07	0.83	8.56
Sc ₂ CF ₂ [50]	e	0.25	1.46	2.26	1.98	193	182	5.03	1.07	4.70	5.62	1.02	5.48	5.62	1.02	5.48
	h(u)	2.25	0.44	1.91	-4.7	193	182	0.48	0.39	1.25	0.61	1.20	2.43	0.42	1.02	1.96
	h(l)	0.46	2.65	-5.0	2.2	193	182	0.31	0.26	1.18	0.94	0.41	2.93	0.78	0.26	2.32
Sc ₂ C(OH) ₂ [50]	e	0.50	0.49	-2.7	-2.6	173	172	2.06	2.19	1.06	2.18	2.22	1.02	2.18	2.22	1.02
	h(u)	5.01	0.27	-3.5	-9.9	173	172	0.05	0.11	2.24	0.02	0.20	11.7	0.02	0.20	11.7
	h(l)	0.29	1.91	-10	-3.2	173	172	0.16	0.24	1.45	0.29	0.07	4.05	0.29	0.07	4.07
Hf ₂ CO ₂ [19]	e	0.23	2.16	10.6	7.10	294	291	0.33	0.08	4.27	0.44	0.06	7.72	0.44	0.06	7.72
	h(u)	0.42	0.16	7.64	2.30	294	291	0.92	26.0	28.1	1.67	7.13	4.28	1.68	7.21	4.26
	h(l)	0.16	0.41	2.02	7.42	294	291	34.3	1.00	34.3	8.04	1.86	4.33	8.14	1.88	4.31
Zr ₂ CO ₂ [19]	e	0.27	1.87	13.9	5.21	265	262	0.15	0.15	1.02	0.26	0.06	4.59	0.26	0.06	4.60
	h(u)	0.16	0.38	9.84	1.80	265	262	1.37	17.5	12.8	2.72	2.20	1.24	2.74	2.21	1.24
	h(l)	0.36	0.16	5.45	6.04	265	262	2.08	3.71	1.78	1.98	4.17	2.10	1.98	4.17	2.10

Note. ‘e’ and ‘h’ denote ‘electron’ and ‘hole’, respectively. m_x and m_y are measured as the ratio with m_0 (the electron mass in vacuum). E_{1x} and E_{1y} are in units of eV. C_{11} and C_{22} are in units of J/m². μ_x and μ_y are in units of 10³ cm²V⁻¹s⁻¹. The values of μ_x , μ_y , E_{1x} , E_{1y} , C_{11} and C_{22} are extracted from references as indicated. μ_x and μ_y are calculated in three ways: (old) same as in original references (largely based Eq. (3)), (new) Eq. (38), and (simplified) Eq. (39). The anisotropic ratio R_{ani} is calculated by Eq. (40). ‘upper’ and ‘lower’ sub-bands in the literature are represented by (u) and (l) here. For few layer samples, for n layer sample, which is expressed as n – sample type, such as n -BP and n – BC₂N.

holes, it predicted that $\mu_x < \mu_y$. However, according to the new formula, the contribution of the deformation potential to the mobility anisotropy is actually weak, and the main contributor is the effective mass. m_x of BP is smaller than m_y , so $\mu_x > \mu_y$ under the new formula. This is consistent with predictions made using the Kubo-Nakano-Mori method based on electron-phonon scattering matrices [54] and charged-

impurity scattering theory [55]. Moreover, this is in agreement with the experimental observations [18,52,53].

TiS₃ monolayer is a new 2D material predicted to possess novel electronic properties [40,41,56]. First-principles calculations showed that TiS₃ is a direct-gap semiconductor with a bandgap of 1.02 eV, close to that of bulk silicon [40]. With the old method, TiS₃ was predicted to possess high

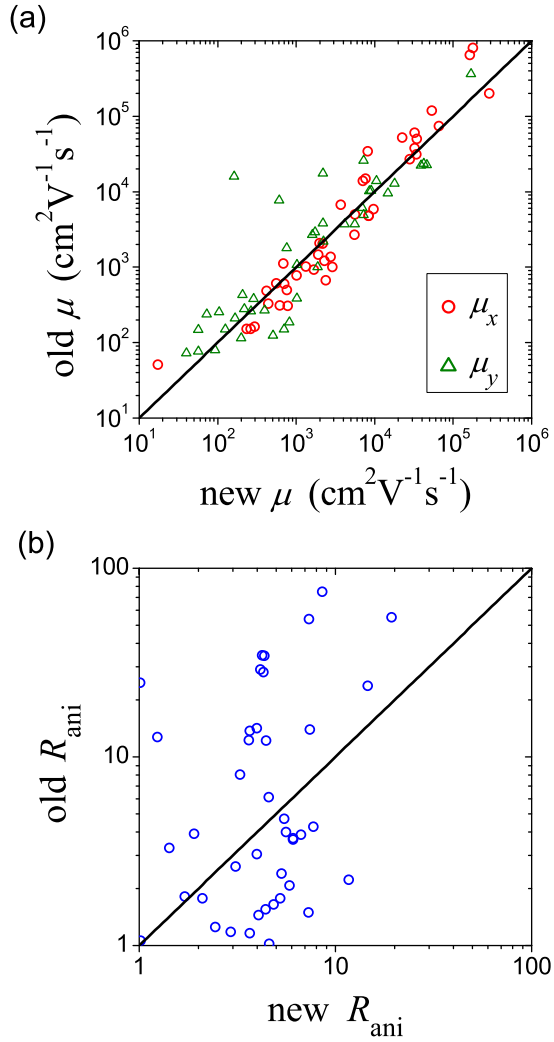


FIG. 3. Comparison between the results for various systems calculated by old and new methods, i.e. Eq. (3) and Eq. (39). (a) The mobility μ_x and μ_y . (b) The anisotropic ratio R_{ani} defined by Eq. (40). Detailed data are provided in Table I.

mobility up to $14 \times 10^3 \text{ cm}^2 \text{V}^{-1} \text{s}^{-1}$ for electrons in the y direction [$\mu_y(\text{e})$], and more remarkably, the mobility is highly anisotropic, i.e., $\mu_y(\text{e})$ is about 14 times higher than $\mu_x(\text{e})$ and is even two orders of magnitude higher than $\mu_y(\text{h})$ [40]. With the new method, however, the obtained anisotropy is much smaller. The re-calculated $\mu_y(\text{e})$ is $10.6 \times 10^3 \text{ cm}^2 \text{V}^{-1} \text{s}^{-1}$, close to the old value, but the re-calculated $\mu_x(\text{e})$ increases from $1.01 \times 10^3 \text{ cm}^2 \text{V}^{-1} \text{s}^{-1}$ to $2.89 \times 10^3 \text{ cm}^2 \text{V}^{-1} \text{s}^{-1}$, giving $R_{\text{ani}} = 3.7$ (see Table I). The recalculated electron/hole mobility ratio is 15, compared with the previously calculated 100, suggesting that the potential in electron/hole separation is not so remarkable as previously thought.

The overall comparison between the results calculated by old and new methods is provided in Fig. 3. The order

of magnitude of μ from the old method is consistent with that from the new method [Fig. 3(a)], although actual values of μ from the two methods differ by a few times. Closer inspection suggests that the deformation potential constant E_1 makes the largest contribution to the resulting discrepancy (data not shown). In contrast, for the calculated anisotropy ratio R_{ani} , there is almost no correlation between the results from old and new methods [Fig. 3(b)], indicating that the old method is highly unreliable in predicting R_{ani} . There are two main reasons for that. First, R_{ani} is determined by ratios of parameters, such as m_x/m_y , C_{11}/C_{22} , and E_{1x}/E_{1y} , but is independent of these individual parameters. As a result, the range of magnitude of R_{ani} is much smaller than that of μ (see Fig. 3). Second, based on Eq. (3) and Eq. (39), when the factor m_x/m_y , C_{11}/C_{22} , or E_{1x}/E_{1y} overestimates (or underestimates) μ_x of a system in the old method (compared with the new method), it would inevitably underestimate (or overestimate) μ_y of the same system. This further amplifies the discrepancy in R_{ani} between old and new methods.

Overall, the old method is more likely to predict high anisotropy. For example among all 42 data points, only three were predicted by the new method to possess $R_{\text{ani}} > 10$: holes of BP (14.6), holes of BC_2N (19.3), and holes of $\text{Sc}_2\text{C}(\text{OH})_2$ (11.7). In comparison, the old method predicted 15 data points to have $R_{\text{ani}} > 10$, three of which possess $R_{\text{ani}} > 50$: holes of BC_2N (54.9), and holes (75.3) and electrons (53.7) of GeCH_3 .

V. SUMMARY

In summary, we theoretically studied the longitudinal acoustic phonon limited mobility for anisotropic 2D semiconductors under the framework of the deformation potential theory. The influences of anisotropic deformation potential constant and elastic modulus were analytically derived. We showed that the mobility in one direction depends not only on the parameters (effective mass, deformation potential constant, and elastic modulus) in the same direction, but also on those in the perpendicular direction. The mobility anisotropy is mainly contributed by the anisotropic effective mass, while the contribution from the deformation potential constant and elastic modulus are much weaker. Parameters for various anisotropic 2D materials were collected for the anisotropic mobility calculation. It was demonstrated that the old formulas widely adopted in the literatures are unreliable and more likely to overestimate R_{ani} when compared with our new formula.

ACKNOWLEDGMENTS

The authors thank Zhenzhu Li, Ting Cheng, and Mei Zhou for helpful discussions. This work was supported by the National Natural Science Foundation of China (Grant No. 21373015).

H.L. and S.Z. contributed equally to this work.

[1] K. S. Novoselov, A. K. Geim, S. V. Morozov, D. Jiang, Y. Zhang, S. V. Dubonos, I. V. Grigorieva, and A. A. Firsov, *Science* **306**, 666 (2004).

[2] A. K. Geim and K. S. Novoselov, *Nat. Mater.* **6**, 183 (2007).

[3] J. Wang, S. Deng, Z. Liu, and Z. Liu, *Natl. Sci. Rev.* **2**, 22 (2015).

- [4] R. P. Feynman, *There is Plenty of Room at the Bottom*, edited by HD Gilbert (Reinhold, New York, 1961).
- [5] D. S. L. Abergel, V. Apalkov, J. Berashevich, K. Ziegler, and T. Chakraborty, *Adv. Phys.* **59**, 261 (2010).
- [6] M. J. Allen, V. C. Tung, and R. B. Kaner, *Chem. Rev.* **110**, 132 (2010).
- [7] K. I. Bolotin, K. J. Sikes, Z. Jiang, M. Klima, G. Fudenberg, J. Hone, P. Kim, and H. L. Stormer, *Solid State Commun.* **146**, 351 (2008).
- [8] S. V. Morozov, K. S. Novoselov, M. I. Katsnelson, F. Schedin, D. C. Elias, J. A. Jaszczak, and A. K. Geim, *Phys. Rev. Lett.* **100**, 016602 (2008).
- [9] I. Meric, M. Y. Han, A. F. Young, B. Ozyilmaz, P. Kim, and K. L. Shepard, *Nat. Nanotechnol.* **3**, 654 (2008).
- [10] G. R. Bhimanapati, Z. Lin, V. Meunier, Y. Jung, J. Cha, S. Das, D. Xiao, Y. Son, M. S. Strano, V. R. Cooper, L. Liang, S. G. Louie, E. Ringe, W. Zhou, S. S. Kim, R. R. Naik, B. G. Sumpter, H. Terrones, F. Xia, Y. Wang, J. Zhu, D. Akinwande, N. Alem, J. A. Schuller, R. E. Schaak, M. Terrones, and J. A. Robinson, *ACS Nano* **9**, 11509 (2015).
- [11] J. Wang, R. Zhao, Z. Liu, and Z. Liu, *Small* **9**, 1373 (2013).
- [12] K. Srinivasu and S. K. Ghosh, *J. Phys. Chem. C* **116**, 5951 (2012).
- [13] G. Li, Y. Li, H. Liu, Y. Guo, Y. Li, and D. Zhu, *Chem. Commun.* **46**, 3256 (2010).
- [14] S. Zhang, J. Wang, Z. Li, R. Zhao, L. Tong, Z. Liu, J. Zhang, and Z. Liu, *J. Phys. Chem. C* **120**, 10605 (2016).
- [15] Y. Cai, G. Zhang, and Y. W. Zhang, *J. Am. Chem. Soc.* **136**, 6269 (2014).
- [16] W. Zhang, Z. Huang, W. Zhang, and Y. Li, *Nano Res.* **7**, 1731 (2014).
- [17] J. Qiao, X. Kong, Z.-X. Hu, F. Yang, and W. Ji, *Nat. Commun.* **5**, 4475 (2014).
- [18] F. Xia, H. Wang, and Y. Jia, *Nat. Commun.* **5**, 4458 (2014).
- [19] X. H. Zha, Q. Huang, J. He, H. He, J. Zhai, J. S. Francisco, and S. Du, *Sci. Rep.* **6**, 27971 (2016).
- [20] X. Zhang, X. Zhao, D. Wu, Y. Jing, and Z. Zhou, *Nanoscale* **7**, 16020 (2015).
- [21] L. Li, Y. Yu, G. J. Ye, Q. Ge, X. Ou, H. Wu, D. Feng, X. H. Chen, and Y. Zhang, *Nat. Nanotechnol.* **9**, 372 (2014).
- [22] R. Fei and L. Yang, *Nano Lett.* **14**, 2884 (2014).
- [23] M. Long, L. Tang, D. Wang, Y. Li, and Z. Shuai, *ACS Nano* **5**, 2593 (2011).
- [24] J. Xi, M. Long, L. Tang, D. Wang, and Z. Shuai, *Nanoscale* **4**, 4348 (2012).
- [25] J. Wu, N. Mao, L. Xie, H. Xu, and J. Zhang, *Angew. Chem. Int. Ed.* **54**, 2366 (2015).
- [26] F. Liu, S. Zheng, X. He, A. Chaturvedi, J. He, W. L. Chow, T. R. Mion, X. Wang, J. Zhou, Q. Fu, H. J. Fan, B. K. Tay, L. Song, R.-H. He, C. Kloc, P. M. Ajayan, and Z. Liu, *Adv. Funct. Mater.* **26**, 1169 (2016).
- [27] E. Liu, Y. Fu, Y. Wang, Y. Feng, H. Liu, X. Wan, W. Zhou, B. Wang, L. Shao, C. H. Ho, Y. S. Huang, Z. Cao, L. Wang, A. Li, J. Zeng, F. Song, X. Wang, Y. Shi, H. Yuan, H. Y. Hwang, Y. Cui, F. Miao, and D. Xing, *Nat. Commun.* **6**, 6991 (2015).
- [28] J. Bardeen and W. Shockley, *Phys. Rev.* **80**, 72 (1950).
- [29] S. Kawaji, *J. Phys. Soc. Jpn.* **27**, 906 (1969).
- [30] M. Kazuo, H. Chihiro, T. Kenji, and I. Masao, *Jpn. J. Appl. Phys.* **28**, 1856 (1989).
- [31] S. Takagi, A. Toriumi, M. Iwase, and H. Tango, *IEEE Trans. Electron Devices* **41**, 2363 (1994).
- [32] J. Xie, Z. Y. Zhang, D. Z. Yang, D. S. Xue, and M. S. Si, *J. Phys. Chem. Lett.* **5**, 4073 (2014).
- [33] G. Schusteritsch, M. Uhrin, and C. J. Pickard, *Nano Lett.* **16**, 2975 (2016).
- [34] T. Satô, Y. Takeishi, H. Hara, and Y. Okamoto, *Phys. Rev. B* **4**, 1950 (1971).
- [35] P. J. Price, *Ann. Phys.* **133**, 217 (1981).
- [36] J. M. Hinckley and J. Singh, *Phys. Rev. B* **42**, 3546 (1990).
- [37] J. E. Northrup, *Appl. Phys. Lett.* **99**, 062111 (2011).
- [38] S. Bruzzone and G. Fiori, *Appl. Phys. Lett.* **99**, 222108 (2011).
- [39] S. Takagi, J. L. Hoyt, J. J. Welser, and J. F. Gibbons, *J. Appl. Phys.* **80**, 1567 (1996).
- [40] J. Dai and X. C. Zeng, *Angew. Chem. Int. Ed.* **54**, 7572 (2015).
- [41] Y. Aierken, D. Cakir, and F. M. Peeters, *Phys. Chem. Chem. Phys.* **18**, 14434 (2016).
- [42] Y. Jing, X. Zhang, D. Wu, X. Zhao, and Z. Zhou, *J. Phys. Chem. Lett.* **6**, 4252 (2015).
- [43] C. H. Park, N. Bonini, T. Sohier, G. Samsonidze, B. Kozinsky, M. Calandra, F. Mauri, and N. Marzari, *Nano Lett.* **14**, 1113 (2014).
- [44] J.-H. Chen, C. Jang, S. Xiao, M. Ishigami, and M. S. Fuhrer, *Nat. Nanotechnol.* **3**, 206 (2008).
- [45] D. K. Efetov and P. Kim, *Phys. Rev. Lett.* **105**, 256805 (2010).
- [46] Z. Li, J. Wang, and Z. Liu, *J. Chem. Phys.* **141**, 144107 (2014).
- [47] F. Han, *A Modern Course in the Quantum Theory of Solids* (World Scientific Publishing Company, Singapore, 2013), pp. 327–371.
- [48] C. Herring and E. Vogt, *Phys. Rev.* **101**, 944 (1956).
- [49] Z. Lin and Z. Liu, *J. Chem. Phys.* **143**, 214109 (2015).
- [50] X. H. Zha, J. Zhou, Y. Zhou, Q. Huang, J. He, J. S. Francisco, K. Luo, and S. Du, *Nanoscale* **8**, 6110 (2016).
- [51] A. Morita, *Appl. Phys. Solid Surface* **39**, 227 (1986).
- [52] L. Li, G. J. Ye, V. Tran, R. Fei, G. Chen, H. Wang, J. Wang, K. Watanabe, T. Taniguchi, L. Yang, X. H. Chen, and Y. Zhang, *Nat. Nanotechnol.* **10**, 608 (2015).
- [53] A. Mishchenko, Y. Cao, G. L. Yu, C. R. Woods, R. V. Gorbachev, K. S. Novoselov, A. K. Geim, and L. S. Levitov, *Nano Lett.* **15**, 6991 (2015).
- [54] A. N. Rudenko, S. Brener, and M. I. Katsnelson, *Phys. Rev. Lett.* **116**, 246401 (2016).
- [55] Y. Liu, T. Low, and P. P. Ruden, *Phys. Rev. B* **93**, 165402 (2016).
- [56] J. O. Island, M. Barawi, R. Biele, A. Almazan, J. M. Clamagirand, J. R. Ares, C. Sanchez, H. S. J. van der Zant, J. V. Alvarez, R. D'Agosta, I. J. Ferrer, and A. Castellanos-Gomez, *Adv. Mater.* **27**, 2595 (2015).